$n:m$ phase synchronization with mutual coupling phase signals

J. Y. Chen and K. W. Wong
Department of Computer Engineering and Information Technology, City University of Hong Kong, Hong Kong, People's Republic of China

J. W. Shuai
Department of Physics and Astronomy, Ohio University, Athens, Ohio 45701

(Received 18 June 2001; accepted 2 January 2002; published 21 February 2002)

We generalize the $n:m$ phase synchronization between two chaotic oscillators by mutual coupling phase signals. To characterize this phenomenon, we use two coupled oscillators to demonstrate their phase synchronization with amplitudes practically noncorrelated. We take the 1:1 phase synchronization as an example to show the properties of mean frequencies, mean phase difference, and Lyapunov exponents at various values of coupling strength. The phase difference increases with 2π phase slips below the transition. The scaling rules of the slip near and away from the transition are studied. Furthermore, we demonstrate the transition to a variety of $n:m$ phase synchronizations and analyze the corresponding coupling dynamics. © *2002 American Institute of Physics.*
[DOI: 10.1063/1.1452738]

The interaction between two or more chaotic oscillators can produce different types of synchronization phenomena, depending on the degree to which the oscillators adjust their motion in accordance with one another. Phase synchronization (PS), i.e., the phase of the oscillators is locked, may play an essential role in the regulation of various biological systems, as well as have potential applications in engineering fields. In this article, we investigate the phase synchronization between two chaotic oscillators with phase coupling. Various ratios of phase synchronization can be found with a variety of coupling strengths. Their dynamical properties are analyzed in detail. Our investigations lead to an alternative way to obtain robust PS that may lead to advancement in the research on nonlinear dynamics.

I. INTRODUCTION

The study of coupled oscillators is a fundamental research interest with applications in various fields.[1–5] In particular, the mutual synchronization of the oscillators is of great interest and importance among the collective dynamics of coupled oscillators. It usually occurs only when the coupling strength is sufficiently large. Various types of synchronization including complete synchronization,[6–8] generalized synchronization,[9–11] and phase synchronization[11–22] have been studied. Among them, the phase synchronization (PS) of chaotic oscillators with mutual coupling of variables usually occurs at coupling strength smaller than that required for complete synchronization. This is because PS corresponds to an entrainment of phases of chaotic oscillators, whereas their amplitudes remain chaotic and noncorrelated. Under classical definition, PS occurs if the difference $|\phi_1-\phi_2|$ between the corresponding phases is bounded by a small preselected constant where $\phi(t)$ is the instantaneous phase of the chaotic oscillator. A weaker synchronization, referred as imperfect PS,[12] is the coincidence of the mean frequencies, i.e., $\Omega_1=\Omega_2$, while their phase differences are unbounded. The mean frequency is defined as $\Omega=\langle\dot{\phi}\rangle$ where $\langle\cdot\rangle$ means averaging over time. On the other hand, for a given system, the degree and rate of synchronization depend vitally on the coupling scheme used. Investigations on PS are usually based on systems with direct state coupling.[12] In order to uncover the properties of PS extensively, some other coupling schemes, such as unidirectional coupling,[20] binary coupling,[21] and asymmetric coupling,[22] have been studied. These schemes can optimize or improve the synchronization among the coupled systems.

For two structurally equivalent systems, i.e., systems where the nonidenticity resulted in a rather small parameter mismatch, a (direct) state coupling can lead to perfect PS between them. However, the PS between two structurally nonequivalent systems is always imperfect and so it is necessary to find an effective coupling scheme that can achieve perfect PS in this case. On the other hand, $n:m$ PS where $n\neq m$ has been found from the firing activities of groups of neurons in human brain.[23] Normally, the state coupling can only achieve 1:1 PS and thus is difficult to fully explain the dynamical approach between groups of neurons. Therefore, the investigation of other coupling ways that can easily obtain $n:m$ PS where $n\neq m$ is also interesting for biological science.

Recently, we studied phase coupling to obtain $n:m$ PS in drive-response Rössler oscillators.[18] Rich behaviors such as amplitude reduction were found. However, this method can only be applied to chaotic oscillators whose attractors have single rotation center, such as Rössler oscillators. In this article, we go further to develop a general phase coupling method. With this method, PS between two general and structurally nonequivalent systems can be obtained by mutual coupling phase signals. Their amplitudes remain noncorrelated even at various coupling strengths. As an example, the dynamics of 1:1 PS is discussed in detail. Before the

transition to PS, the phase difference increases with 2π phase slips. When the coupling strength approaches the transition to PS, the distribution of laminar length changes from a single normal distribution to two periods of normal distribution and then to Lorentzian shapes. Here, the laminar length is defined as the time elapsed between two successive 2π phase slips.[16] For a better understanding of the coupling dynamics, the mean phase difference, the mean frequencies and the Lyapunov exponents at various values of coupling strength are also studied. Moreover, we demonstrate the transition to PS at various $n:m$ ratios. The coupling dynamics that influence the values of transition is also discussed. Our investigation leads to an alternative way to obtain robust $n:m$ PS that may benefit the advancement of nonlinear dynamics.

This article is organized as follows. In Sec. II, the dynamical properties of two coupled oscillators with phase coupling are introduced. In order to examine the proposed method, we take two coupled Rössler and Lorenz oscillators as an example to show the $n:m$ PS in Sec. III. PS transition as well as phase slips near and away from the transition are discussed in detail. Furthermore, we consider, in Sec. IV, the coupled chaotic Rössler and hyperchaotic Rössler oscillators as another example. The results show that the PS with phase coupling is perfect even for structurally nonequivalent systems. In Sec. V, we claim that the phase coupling can be extended to a scalar of coupled oscillators so as to achieve global PS. The differences between state coupling and phase coupling are discussed. The potential applications of phase coupling are also pointed out. Finally, our conclusions are drawn in the last section.

II. DYNAMICAL PROPERTIES OF TWO COUPLED OSCILLATORS WITH PHASE COUPLING

Most autonomous chaotic oscillators can be represented in the form

$$\dot{X}=F(X). \tag{1}$$

Here, $\dot{X}$ can be considered as the speed vector of the trajectory in the phase plane. If a parameter is added to Eq. (1), the equation becomes

$$\dot{X}=\eta F(X). \tag{2}$$

Here $\eta>0$ gives the parametrization of time. For neural dynamics, such as the FitzHugh–Nagumo oscillator,[24] η is the characteristic time scale of the activator and inhibitor. By this means, the oscillator dynamics can be interpreted as follows. As the magnitude of the Lyapunov exponents reflects the time scale on which the oscillator dynamics become unpredictable[25] and that η could also be considered as the coefficient of the oscillator's time scale, magnitude of the Lyapunov exponents should be directly proportional to η. For example, suppose that the ith Lyapunov exponent of Eqs. (1) and (2) is represented by λ_i^{Nat} and λ_i, respectively. (In this article, if the dynamical quantities are obtained from $\eta\equiv 1$, they are marked with the superscript "Nat.") They are defined in terms of the length of the ellipsoidal principal axis p_i and both principals increase from the same initial value $p_i(0)$. They could be written, respectively, as

$$\lambda_i^{\mathrm{Nat}}=\lim_{T\to\infty}\frac{1}{T}\ln\frac{p_i(T)}{p_i(0)} \tag{3}$$

and

$$\lambda_i=\lim_{T\to\infty}\frac{1}{T'}\ln\frac{p_i(T')}{p_i(0)}, \tag{4}$$

where λ_i^{Nat} and λ_i are both arranged from the largest to the smallest with index i. If $p_i(T')=p_i(T)$, their time duration should be $T'=T/\eta$. Comparing Eqs. (3) and (4), their Lyapunov exponents have the relationship

$$\lambda_i=\eta\lambda_i^{\mathrm{Nat}}. \tag{5}$$

As η is the time scale coefficient, the trajectory of Eq. (2) has the same geometric structure at different η's. Different values of η only relate to different rotation speed on the same trajectory represented by phase and mean frequency. Comparing with Eq. (1), the corresponding phase and mean frequency of Eq. (2) have the following forms:

$$\phi(t)=\eta\phi^{\mathrm{Nat}}(t) \tag{6}$$

and

$$\Omega=\eta\Omega^{\mathrm{Nat}}. \tag{7}$$

In order to achieve the mutual coupling of phase signals, η can be transformed to a dynamical quantity determined by the interaction of both frequencies and the locking ratio $n:m$. The quantity can be interpreted as $\eta(t)=G(n\phi_1,m\phi_2)$ where the function $G(\cdot)$ is constructed to have the following properties. If $n\phi_1>m\phi_2$, $0<\eta<1$. However, if $n\phi_1<m\phi_2$, $\eta>1$. As a result, the $n:m$ PS could be obtained with the following form:

$$\dot{X}=\eta(t)F_1(X) \tag{8}$$

and

$$\dot{Y}=\eta^{-1}(t)F_2(Y). \tag{9}$$

Here $F_1(X)$ and $F_2(Y)$ can be two different oscillators. From the above description of $G(\cdot)$, the interactions of Eqs. (8) and (9) have the following feedback: When $n\phi_1>m\phi_2$, $\eta<1$ in Eq. (8) and therefore $\eta^{-1}>1$ in Eq. (9). Hence, $\dot{\phi}_1\downarrow$ and $\dot{\phi}_2\uparrow$ implies $\dot{\phi}_1\approx\dot{\phi}_2$. On the other hand, if $n\phi_1<m\phi_2$, a similar feedback mechanism can also result in $\dot{\phi}_1\approx\dot{\phi}_2$. Evidently, the function of $G(\cdot)$ is not unique and it is not difficult to construct a suitable function with the above properties. In this article, we define the coupling term as $\eta(t)=\exp(\epsilon\sin\theta)$ with $\epsilon\geqslant 0$. It is interpreted as follows: The phase difference is $\theta(t)=n\phi_2(t)-m\phi_1(t)$ with phase ratio $n:m$. As the parameter ϵ is related to the strength of coupling, it is called the coupling strength. In general, the phase difference is in the range of $-\infty<\theta<\infty$ and so it could not be used directly. A sine function is thus imposed to obtain the new range $-1\leqslant\sin\theta\leqslant 1$. A natural exponent in η guarantees a positive control parameter with various phase differences.

The mutual coupling of phase signals can influence their rotation speeds. Suppose that $0<\theta<\pi/2$ at time t. This means that the phase $n\phi_2$ of Eq. (9) is in advance of the phase $m\phi_1$ of Eq. (8). Thus we obtain $\eta>1$ which indicates that the rotation speed of Eq. (8) is faster while that of Eq. (9) is slower. The phase difference θ will reduce in their subsequent time. In this case, the interactive coupling η acts as a negative feedback to drive the phase difference to converge. Similar discussion shows that the negative feedback is within the range of $2\pi k-\pi/2\leqslant\theta\leqslant 2\pi k+\pi/2$ with integer k. While in the range of $2\pi k+\pi/2\leqslant\theta\leqslant 2\pi k+3\pi/2$, the feedback becomes positive and it may introduce phase slips to enter the adjacent negative feedback region. When ϵ exceeds a transition value, θ is located in the negative feedback region with a small amplitude fluctuation and so the $n:m$ PS can be obtained.

For the coupling systems defined by Eqs. (8) and (9), $\eta(t)$ varies with time. It can be written as $\eta(t)=\langle\eta\rangle+\xi(t)$ where ξ represents a fluctuation with zero mean. Using adiabatic approach,[26] we have

$$\langle\eta(\epsilon)\rangle=\langle\exp(\epsilon\ \sin\ \theta)\rangle\approx\exp(\epsilon\ \sin\langle\theta\rangle). \tag{10}$$

In this article, if not specified, the mean phase difference $\langle\theta\rangle$ is always obtained from $-2\pi\leqslant\theta\leqslant 2\pi$ with $|\theta|\mathrm{mod}2\pi$ because $\pm 2k\pi$ contributes nothing to sin θ. As Ω is obtained from a long time average, ξ can be neglected. By this means, when $\epsilon>0$, Eq. (7) gives the following relationships:

$$\Omega_1(\epsilon)\approx\langle\eta(\epsilon)\rangle\Omega_1^{\mathrm{Nat}} \tag{11}$$

and

$$\Omega_2(\epsilon)\approx\langle\eta^{-1}(\epsilon)\rangle\Omega_2^{\mathrm{Nat}}. \tag{12}$$

The Lyapunov exponents are also obtained from a long time average of the increment of the system's ellipsoidal principals shown in Eq. (4). Thus, according to Eq. (5), we can obtain the following Lyapunov exponents for the coupled oscillators given by Eqs. (8) and (9):

$$\lambda_i\approx\langle\eta\rangle\lambda_i^{\mathrm{Nat}}. \tag{13}$$

When the coupling strength exceeds a transition value, their instantaneous phases are at $n:m$ PS. Then the mean frequencies correspond to $\Omega_1^{\mathrm{PS}}(\epsilon)$ and $\Omega_2^{\mathrm{PS}}(\epsilon)$ with $m\Omega_1^{\mathrm{PS}}(\epsilon)=n\Omega_2^{\mathrm{PS}}(\epsilon)$. As a result, one can get, at $n:m$ PS,

$$\langle\eta^{\mathrm{PS}}\rangle\approx\eta_0 \tag{14}$$

with

$$\eta_0=\sqrt{(n\Omega_2^{\mathrm{Nat}})/(m\Omega_1^{\mathrm{Nat}})}. \tag{15}$$

It suggests that the time average of dynamical quantity η is independent of ϵ after PS. This means that the mean frequencies and the Lyapunov exponents of coupled oscillators described by Eqs. (8) and (9) remain constant at various values of coupling strength after PS.

III. COUPLED RÖSSLER AND LORENZ OSCILLATORS WITH PHASE COUPLING

If the two different oscillators are coupled by state variables, it is difficult to find perfect 1:1 PS. This is because the method can only be used in oscillators with similar dynamics and mean frequencies, such as two coupled Rössler oscillators with a small parameter mismatch.[17] For two structurally nonequivalent oscillators, such as the case of a coupling between a chaotic and a hyperchaotic Rössler system,[12] or the case of a coupling between two coupled Mackey–Glass equations with two different time delays,[29] only imperfect PS can be found.

We take the phase coupling of two different oscillators, Lorenz and Rössler, as an example to demonstrate the $n:m=1:1$ PS phenomena in detail. Then the PS phenomena with various locking ratios are described briefly. The coupled Rössler oscillator is governed by the following equations:[27]

$$\begin{aligned}\dot{x}_1&=\eta(t)\cdot(-y_1-z_1),\\ \dot{y}_1&=\eta(t)\cdot(x_1+0.15y_1),\\ \dot{z}_1&=\eta(t)\cdot[0.2+z_1(x_1-10)].\end{aligned} \tag{16}$$

And the corresponding equations for the coupled Lorenz oscillator are[28]

$$\begin{aligned}\dot{x}_2&=\eta^{-1}(t)\cdot 10(y_2-x_2),\\ \dot{y}_2&=\eta^{-1}(t)\cdot(36.5x_2-y_2-x_2z_2),\\ \dot{z}_2&=\eta^{-1}(t)\cdot(-3.0z_2+x_2y_2),\end{aligned} \tag{17}$$

where the dynamical quantity $\eta(t)=\exp(\epsilon\ \sin\ \theta(t))$ with $\theta(t)=\phi_2(t)-\phi_1(t)$ and $\epsilon\geqslant 0$. For simplicity, we utilize the reflection symmetry ($x_2\leftrightarrow -x_2$ and $y_2\leftrightarrow -y_2$) of the Lorenz attractor. A new variable $u=\sqrt{x_2^2+y_2^2}$ is defined so that a phase can be suitably defined on the $u-z$ plane with the rotation center $(u_0,z_0)\rightarrow(15,36)$.[17] We can easily obtain the phase $\phi_2=\arctan[(z_2-z_0)/(u-u_0)]$ for Lorentz oscillator and $\phi_1=\arctan(y_1/x_1)$ for Rössler oscillator.

The two oscillators in our example have different scales of mean frequencies at uncoupled states. They are $\Omega_1^{\mathrm{Nat}}=1.034$ and $\Omega_2^{\mathrm{Nat}}=10.23$, respectively. That is to say, the mean frequency of Lorentz oscillator is ten times higher than that of the Rössler one. However, PS can still be achieved by using our method. The coupling strength at PS transition is about $\epsilon_c=1.38$, which is marked by a dotted line γ in Fig. 1. Dynamics of the coupling term η in the achievement of PS between two coupled oscillators is rather complex. In the following, several simulations are performed to analyze the nontrivial characteristics of the coupled oscillators by statistical means. According to Eq. (10), the mean value of $\eta(t)$ is determined by $\langle\theta\rangle$. Figure 1(a) shows the curve of $\langle\theta\rangle$ and the corresponding $\langle\eta\rangle$ at various values of ϵ. Let us first focus on the region after the transition. The curve of $\langle\theta\rangle$ goes down monotonically in this region and the corresponding $\langle\eta\rangle$ is close to the dash line $\eta_0(=3.15)$. This implies that the simulation results confirm the analytical result given by Eq. (14). Near the transition, the curve of $\langle\theta\rangle$ has a small fluctuation that is produced by the occasional 2π phase slips. We will discuss this phenomenon later. Figures 1(b) and 1(c) show the mean frequencies and the Lyapunov exponents at various ϵ. These curves match the dynamics properties described by Eqs. (11)–(13). At the transition, the mean frequency is $\Omega^{\mathrm{PS}}=3.25$. It approximately equals to the value of $\Omega_1^{\mathrm{Nat}}/\eta_0$ or $\Omega_2^{\mathrm{Nat}}\eta_0$. The corresponding two largest Lyapunov exponents are $\lambda_1=0.38$ and $\lambda_2=0.29$, respec-

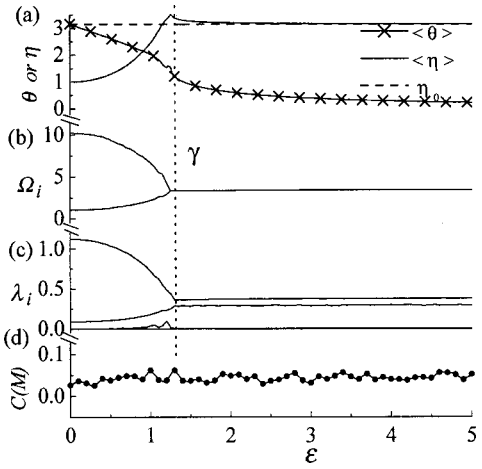

FIG. 1. (a) The mean phase difference $\langle\theta\rangle$, $\langle\eta\rangle$, and η_0. (b) The mean frequency of Ω_1 and Ω_2. (c) The four largest Lyapunov exponents λ_i ($i=1,2,3,4$). (d) The maximum of normal cross-correlation $C(M)$ of the two coupled oscillators versus the coupling strength ϵ. The vertical dotted line γ indicates the PS transition ϵ_c.

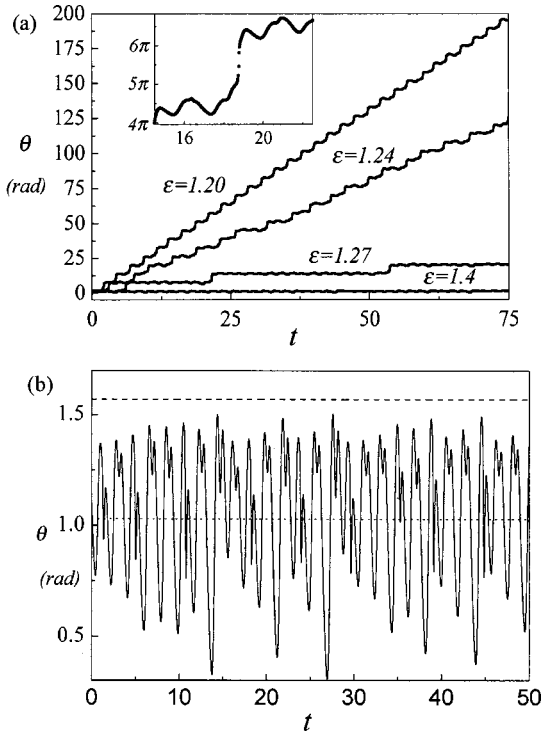

FIG. 2. (a) Time evolutions of phase difference θ in two coupled Rössler and Lorenz attractors at various values of ϵ. The inset shows an enlargement of a single 2π phase slips appeared on the curve corresponding to $\epsilon=1.24$. (b) The phase difference with small amplitude fluctuation at PS transition. The dotted line refers to the value of mean phase difference while the dashed line is located at $\pi/2$.

tively. They are also approximately equal to the values of $\lambda_1^{\mathrm{Nat}}/\eta_0$ and $\lambda_2^{\mathrm{Nat}}\eta_0$ where $\lambda_1^{\mathrm{Nat}}=1.12$ and $\lambda_2^{\mathrm{Nat}}=0.092$ at $\epsilon=0$. However, these dynamical quantities have some small mismatches at the transition. In Fig. 1(a), there is a relative large mismatch between the values of $\langle\eta\rangle$ and η_0. Moreover, in Fig. 1(b), the point where the mean frequency approaches Ω^{PS} is slightly earlier than the dotted line γ. This is because the transition to PS is always smeared and observed only as a tendency, or as a temporary event in some finite time intervals.[16] After the PS transition, the mean frequency and the two largest Lyapunov exponents remain constant. For the two zero Lyapunov exponents, only one of them has little fluctuation near the PS transition. Similar to the case of the mean phase difference, it may be the occasionally 2π phase slips that make the coupled oscillators unstable.

As η is a time scale parameter, it only relates to different rotation speed of the trajectory. Therefore, with the coupling method, their amplitudes keep noncorrelated at various values of coupling strength. This can be shown by Fig. 1(d). The normal cross-correlation between two amplitudes are measured using the following formula:[6]

$$C(\tau)=\frac{\langle\overline{A}_1(t)\overline{A}_2(t+\tau)\rangle}{(\langle\overline{A}_1^2(t)\rangle\langle\overline{A}_2^2(t)\rangle)^{1/2}}, \tag{18}$$

where $\overline{A}=A-\langle A\rangle$. The two amplitudes correspond to Eqs. (16) and (17) are $A_1=\sqrt{(u-u_0)^2+(z_2-z_0)^2}$ and $A_2=\sqrt{x_1^2+y_1^2}$, respectively. We plot $C(M)$ which is the maximum of $C(\tau)$ for all τ, versus the coupling strength ϵ. With the increase of ϵ, the value of $C(M)$ is approximately constant. It is around 0.05 which is the same as that at uncoupled state $\epsilon=0$. That is to say, the amplitudes keep noncorrelated all the way because the control method relies on the phases of the two oscillators rather than their state variables. It is different from the observation that, for two chaotic oscillators coupling with variables, their cross-correlation increases with the enlargement of coupling strength after PS.[13]

Similar to the mutual coupling using state variables[17] and phase coupling in drive-response systems,[18] the phase difference appears 2π phase slips near the transition to PS. The time evolution of θ at various values of ϵ is plotted in Fig. 2(a). It shows that θ increases with a nearly periodic laminar length at $\epsilon=1.2$. When $\epsilon=1.24$, the laminar length is extended and appears more than one period. One of the 2π phase slips is enlarged and shown in the inset. Furthermore, when $\epsilon=1.27$, which is near the phase transition, the laminar length shows a sequence of intermittence. When $\epsilon>\epsilon_c$ (≈ 1.38), the phase difference is at a nearly constant mean value with a high-frequency but low-amplitude fluctuation. To observe the fluctuation clearly, the value of θ at the transition to PS is plotted in Fig. 2(b). The dotted and the dashed lines correspond to the mean of the phase difference and $\pi/2$, respectively. Evidently, $\theta_{\max}<\pi/2$ but the difference is not substantial. If $\epsilon<\epsilon_c$, the situation $\theta_{\max}>\pi/2$ occurs which may result in the 2π phase slips.

In an attempt to quantify the difference in the dynamics of phase slips near and away from the transition, we have computed the probability distribution $p(l)$ at various values of coupling strength ϵ. The results are plotted in Fig. 3, where l is the laminar length. Figure 3(a) shows two $p(l)$'s at a coupling strength far away from the transition. Their statistics follow very closely that of a normal distribution. With the increase of ϵ, the single normal distribution splits into two, as observed in Fig. 3(b). Furthermore, the phenomenon changes dramatically when the system approaches the close vicinity of the transition point as shown in Fig. 3(c). The

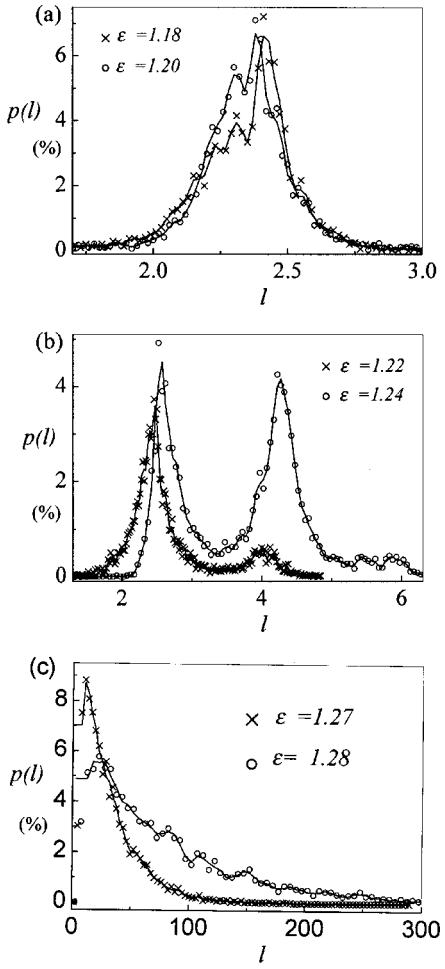

FIG. 3. Probability distribution function $p(l)$ of the 2π phase slips versus the laminar length l with (a) normal distribution, (b) two periods of normal distribution, and (c) a Lorentzian shape.

normal distributions can no longer be retained. Instead, they become a Lorentzian shape. The bandwidth becomes much broader as ϵ moves closer to ϵ_c. Some of these properties are different from that coupled by state variables. In the latter case, the distribution of $p(l)$ changes from a normal shape to a Lorentzian one directly when ϵ moves towards ϵ_c.[17] While the additional two normal distributions of $p(l)$ can be found with our method, the difference may be induced by different coupling mechanisms. With the method coupled by state variables, the coupling strength always corresponds to weak coupling where the mutual systems have close mean frequencies at uncoupled state. The phase slips are mainly caused by the amplitude fluctuations at weak coupling. However, phase coupling is used in our method and the phase slips occur at strong coupling where the mutual systems are different. The mechanism to phase slips becomes more complex so that the additional phenomenon with two normal distribution occurs. But both methods give a Lorentzian shape in the distribution $p(l)$ near the transition. This property indicates that both the transitions to PS are smear.

The proposed coupling method can realize PS easily not only at ratio 1:1, but also at various $n:m$ ratios. For example, set $\beta=m/n$ with $\theta=\phi_2-\beta\phi_1$ for Eqs. (16) and (17) and perform the simulations. The transition to PS ϵ_c, as well as the corresponding $\langle\theta\rangle$, $\langle\eta\rangle$, and $\langle\eta_0\rangle$ are plotted in Fig. 4. In this example, Ω_2^{Nat} is about ten times higher than Ω_1^{Nat} and $\Omega_1\approx\beta\Omega_2$ at phase locking. From Eq. (15), with the increase of β, η_0 is reduced smoothly. Simulations show that at the transition, $\langle\eta\rangle\cong\eta_0$ at various values of β. For the special case that $\beta\approx\Omega_2^{\mathrm{Nat}}/\Omega_1^{\mathrm{Nat}}$, $\eta_0\approx 1$ (as indicated by a dotted line μ_2 in the figure), i.e., their mean frequencies remain unchanged at various coupled strengths. The instantaneous value of η only produces the coherence of their frequency fluctuations to avoid occasional phase slips. When $\beta>\Omega_2^{\mathrm{Nat}}/\Omega_1^{\mathrm{Nat}}$, we need to accelerate the frequency of Eq. (17) instead of that of Eq. (16). Therefore, $\eta_0<1$ and $\langle\theta\rangle<0$.

At the special case marked by μ_2, it is natural to consider that the corresponding ϵ_c also appears global minimum because the mean frequency is unchanged at various coupling strength. However, the global minimum is at μ_1 which is far away from μ_2. This is because the value of ϵ_c is not only influenced by the mismatch of mean frequencies, but also by the coherence of their phases. We can describe the dynamics of phase as[30,31]

$$\dot{\phi}=\Omega+F(A). \tag{19}$$

Here, $F(A)$ is the effective noise with zero mean value that produces phase diffusion and A is its amplitude. For two coupled oscillators, a generalization of Eq. (19) reads

$$\frac{d\theta}{dt}=\Delta\Omega^{\mathrm{Nat}}+\Delta F^{\mathrm{Nat}}+\epsilon G(\theta), \tag{20}$$

with $\Delta\Omega^{\mathrm{Nat}}=\Omega_2^{\mathrm{Nat}}-\beta\Omega_1^{\mathrm{Nat}}$, $\Delta F^{\mathrm{Nat}}=F_2^{\mathrm{Nat}}(A_2)-\beta F_1^{\mathrm{Nat}}(A_1)$ and G describing coupling between two oscillators. As $F_1^{\mathrm{Nat}}(A_1)$ and $F_2^{\mathrm{Nat}}(A_2)$ are independent effective noise, the maximum of interactive frequency fluctuations can be written as $|\Delta F^{\mathrm{Nat}}|_{\max}=|F_1^{\mathrm{Nat}}(A_1)|_{\max}+\beta|F_2^{\mathrm{Nat}}(A_2)|_{\max}$. Although it is difficult to develop a formal mathematical model to interpret the values of ϵ_c at various β, we can clearly find out the properties of ϵ_c at some special cases. Evidently, the fluctuation of θ is mainly produced by ΔF^{Nat} and the increase of ϵ can make ϵG countervail both $\Delta\Omega^{\mathrm{Nat}}$ and ΔF^{Nat}. Moreover, to avoid 2π phase slips at PS, the phase difference requires $|\theta|<\pi/2$. By this means, if $\Delta\Omega^{\mathrm{Nat}}\gg|\Delta F^{\mathrm{Nat}}|_{\max}$, ϵ_c is mainly determined by $\Delta\Omega^{\mathrm{Nat}}$ with $\epsilon_c\propto\Delta\Omega^{\mathrm{Nat}}$. However, if $\Delta\Omega^{\mathrm{Nat}}\ll|\Delta F^{\mathrm{Nat}}|_{\max}$, the main factor turns to ΔF^{Nat} with $\epsilon_c\propto|\Delta F^{\mathrm{Nat}}|_{\max}$. In Fig. 4, when $\beta=1$, ϵ_c is mainly determined by a relative large $\Delta\Omega^{\mathrm{Nat}}$. With the increase of β, $\Delta\Omega^{\mathrm{Nat}}$ reduces. The corresponding ϵ_c diminishes but $|\Delta F^{\mathrm{Nat}}|_{\max}$ increases at the same time. At certain β, the two contrary forces on ϵ_c make its values a global minimum, as indicated by μ_1. When β exceeds μ_1, $\Delta\Omega^{\mathrm{Nat}}$ turns to a small value. As a result, ϵ_c is mainly determined by $|\Delta F^{\mathrm{Nat}}|_{\max}$ and is enlarged along with β. By this means, it is reasonable that the global minimum of ϵ_c is not at the position μ_2 where $\Delta\Omega^{\mathrm{Nat}}=0$.

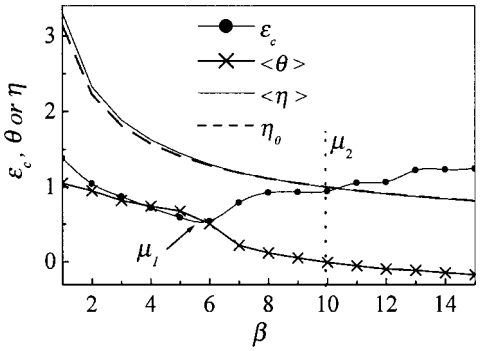

FIG. 4. The coupling strength at the transition ϵ_c, and the corresponding $\langle\theta\rangle$, $\langle\eta\rangle$, and η_0 values at various locking ratio β. The position μ_1 is the global minimum of ϵ_c and the dotted line μ_2 corresponds to $\langle\eta\rangle\approx 1$ and $\langle\theta\rangle\approx 0$.

IV. COUPLED CHAOTIC RÖSSLER AND HYPERCHAOTIC RÖSSLER OSCILLATORS WITH PHASE COUPLING

Comparing with state coupling, a significant characteristic of phase coupling is that perfect PS can always be obtained between two structurally nonequivalent oscillators. We use coupled chaotic Rössler and hyperchaotic Rössler oscillators as another example to show this. The coupled oscillators have been simulated in Ref. 12 using state coupling method. The results show that only imperfect PS can be found, i.e., their mean frequency difference $\Delta\Omega\approx 0$ and the phase difference $\phi_1-\phi_2$ exhibit an unbounded random-type walk. Equations of the coupled oscillators are as follows:[27]

$$\begin{aligned}
\dot{x}_1 &= \eta(t)(-\omega y_1 - z_1),\\
\dot{y}_1 &= \eta(t)(\omega x_1 + 0.15 y_1),\\
\dot{z}_1 &= \eta(t)[0.2 + z_1(x_1 - 10)],\\
\dot{x}_2 &= \eta^{-1}(t)(-y_2 - z_2),\\
\dot{y}_2 &= \eta^{-1}(t)(x_2 + 0.25 y_2 + w),\\
\dot{z}_2 &= \eta^{-1}(t)(3 + x_2 z_2),\\
\dot{w} &= \eta^{-1}(t)(-0.5 z_2 + 0.05 w),
\end{aligned} \tag{21}$$

where the formula of $\eta(t)$ is the same as the example in Eqs. (16) and (17). Parameter ω is the natural frequency that determines the mean frequency of the Rössler oscillator. Details of the instantaneous phase ϕ_2 of the hyperchaotic Rössler oscillator have been discussed in Ref. 16. We mainly focus on the $n:m=1:1$ PS. The mean frequency difference versus ω at various coupling strengths is plotted in Fig. 5(a). With the increase of coupling strength, the regions for PS extend that correspond to the zero of $\Delta\Omega$. The synchronization is perfect PS because their phase difference is bounded at PS region. The bounded phase difference can be explicitly found in Fig. 5(b). The bound $|\Delta\phi|_{\max}$ in Fig. 5(b) corresponds to the PS region in Fig. 5(a). The value of $|\Delta\phi|_{\max}$ increases when ω is away from the center value of natural frequency, i.e., $\omega\approx 0.92$. This is because the mismatch of mean frequencies $\Delta\Omega^{\mathrm{Nat}}$ between $\Omega_1^{\mathrm{Nat}}(\omega)$ and Ω_2^{Nat} increases. When ω is near the transitions from PS to non-PS, the bound $|\Delta\phi|_{\max}$ appear several jumps. They correspond to the phase slips.

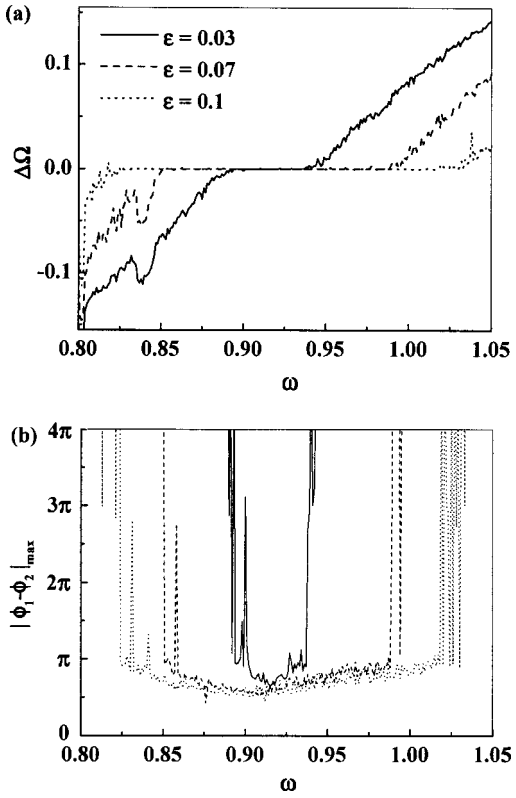

FIG. 5. (a) The mean frequency difference $\Delta\Omega$ in Eqs. (21) and (b) the maximum absolute phase difference $|\Delta\phi|_{\max}$ versus ω at several values of the coupling strength ϵ.

The dynamics for the structurally nonequivalent oscillators have explicit differences. For example, in Eq. (21), the variables of the two oscillators have two different ranges, $-128.6<x_1(t)<20.4$ and $-14.6<x_2(t)<17.3$, respectively. As state coupling directly uses the difference of their corresponding state variable as a weak feedback component, the variable with a large difference can be described with a sufficiently large effective noise which produce unbounded phase difference.[12,30,31] However, their dynamical difference is trivial when phase coupling is used. If both the instantaneous phases can be obtained, perfect PS can be achieved when the coupling strength exceeds a transition.

V. DISCUSSION

As the investigation of networks is essential to all branches of science,[32] the phase coupling can also be applied in a network of coupled oscillators so as to achieve phase locking among the oscillators. For example, we can use $\dot{X}_i = \exp(\epsilon \sin\theta_i) F_i(X_i)$ to obtain global PS where the phase difference is defined as $\theta_i = \langle\phi\rangle - \phi_i$ with $i=1,2,3,\ldots$. The mechanism is similar to that discussed above.

The dynamics of phase coupling is different from that of state coupling. In the latter case, it belongs to the framework of chaos control theory.[33,34] Besides PS, the oscillator dynamics may change from chaos to period under the weak perturbations of the state coupling. While in the former case,

the phenomena are closely related to phase-locking loops (PLL) that are highly relevant to engineering applications.[35] The chaotic dynamics of coupled systems are maintained except the interactive of both frequencies. When a coherent summation is necessary for the outputs of structurally nonequivalent generators whose dynamics have great difference, phase coupling is a better choice to achieve perfect PS because the state coupling can only get imperfect PS, as shown in Sec. IV. The $n:m$ perfect PS of phase coupling may also be an important consideration in schemes for communication using the natural symbolic dynamics of chaos.[36,37] The clock timing of information bits is typically a key factor in a communication system. Therefore, a robust frequency control for chaotic systems is crucial in an application to encoded and decoded communication. Especially, the parameter for phase coupling, i.e., η in Eq. (2), exactly corresponds to the parametrization time due to the hardware of the analog computer.[24] By this means, similar to the PS in state coupling, the $n:m$ PS can also be easily realized in engineering.

PS has been considered as a possible communicating way in biological neural networks.[23,38–40] Investigation of coupling methods among neural systems is important to uncover some properties of nerve activities. Different from state coupling where only 1:1 PS can be achieved, the phase coupling can realize various ratios of PS as required. As $n:m$ PS can also be found in different groups of neural activation,[23] the state coupling is insufficient to explain the various $n:m$ PS in different groups of neural activation. Especially, the dynamics of different groups of neurons are always different. Phase coupling can achieve perfect PS between different dynamical systems because the coupling method only concerns the time scale. Therefore, despite state coupling, phase coupling may also benefit the investigation of the coupling among biological neurons.

VI. CONCLUSION

In conclusion, we have developed an effective way to obtain PS between two interacting chaotic oscillators. As a result, PS of the two coupled oscillators, Lorenz and Rössler, is studied in detail. Furthermore, we use the coupling between chaotic Rössler and hyperchaotic Rössler oscillators as another example to show that the phase coupling can achieve perfect PS between two structurally nonequivalent oscillators. Our method could easily be extended to a scalar of oscillators so as to obtain global PS in the same way. It may be an effective way to investigate the coupling phenomena in various physical and biological fields.

ACKNOWLEDGMENTS

The work described in this article was fully supported by a grant from the Research Grants Council of the Hong Kong Special Administrative Region, China (Project No. CityU 1072/98E).

[1] Y. Kuramoto, *Chemical Oscillations, Waves and Turbulence* (Springer, Berlin, 1984).
[2] B. Blasius, A. Huppert, and L. Stone, Nature (London) **399**, 354 (1999).
[3] K. Otsuka and R. Kawai, Phys. Rev. Lett. **84**, 3049 (2000).
[4] J. N. Blakely, D. J. Gauthier, G. Johnson, T. L. Carroll, and L. M. Pecora, Chaos **10**, 738 (2000).
[5] V. Dronov and E. Ott, Chaos **10**, 291 (2000).
[6] G. Hu, J. H. Xiao, J. Z. Yang, F. G. Xie, and Z. L. Qu, Phys. Rev. E **56**, 2738 (1997).
[7] J. Y. Chen, K. W. Wong, and J. W. Shuai, Phys. Lett. A **263**, 315 (1999).
[8] W. Wang, I. Z. Kiss, and J. L. Hudson, Chaos **10**, 248 (2000).
[9] N. F. Rulkov, M. M. Sushchik, and L. S. Tsimring, Phys. Rev. E **51**, 980 (1995).
[10] L. M. Pecora, T. L. Carroll, G. A. Johnson, D. J. Mar, and J. F. Heagy, Chaos **7**, 520 (1997).
[11] D. Y. Tang, R. Dykstra, M. W. Hamiton, and N. R. Heckenberg, Chaos **8**, 697 (1998).
[12] M. G. Rosenblum, A. S. Pikovsky, and J. Kurths, Phys. Rev. Lett. **76**, 1804 (1996).
[13] J. W. Shuai and D. M. Durand, Phys. Lett. A **264**, 289 (1999).
[14] D. E. Postnov, T. E. Vadivasova, O. V. Sosnovtseva, A. G. Balanov, V. S. Anishchenko, and E. Mosekilde, Chaos **9**, 227 (1999).
[15] V. Andrade, R. L. Davidchack, and Y. C. Lai, Phys. Rev. E **61**, 3230 (2000).
[16] I. Kim, C. M. Kim, W. H. Kye, and Y. J. Park, Phys. Rev. E **62**, 8826 (2000).
[17] K. J. Lee, Y. Kwak, and T. K. Lim, Phys. Rev. Lett. **81**, 321 (1998).
[18] J. Y. Chen, K. W. Wong, H. Y. Zheng, and J. W. Shuai, Phys. Rev. E **63**, 036214 (2001).
[19] A. Pikovsky, M. Zaks, M. Rosenblum, G. Osipov, and J. Kurths, Chaos **7**, 680 (1997).
[20] D. Pazó, I. P. Marino, V. P. Villar, and V. P. Munuzuri, Int. J. Bifurcation Chaos Appl. Sci. Eng. **10**, 2533 (2000).
[21] U. Parlitz and I. Wedekind, Int. J. Bifurcation Chaos Appl. Sci. Eng. **10**, 2527 (2000).
[22] Z. G. Zheng, G. Hu, and B. B. Hu, Phys. Rev. E **62**, 7501 (2000).
[23] P. Tass, M. G. Rosenblum, J. Weule, J. Kurths, A. Pikovsky, J. Volkmann, A. Schnitzler, and H. J. Freund, Phys. Rev. Lett. **81**, 3291 (1998).
[24] U. Parlitz, L. Junge, W. Lauterborn, and L. Kocarev, Phys. Rev. E **54**, 2115 (1996).
[25] A. Wolf, J. B. Swift, H. L. Swinney, and J. A. Vastano, Physica D **16**, 285 (1985).
[26] D. J. Amit, *Modeling Brain Function: The World of Attractor Neural Networks* (Cambridge University Press, Cambridge, 1989).
[27] O. E. Rossler, Phys. Lett. A **57**, 397 (1976).
[28] E. N. Lorenz, J. Atmos. Sci. **20**, 155 (1979).
[29] S. Boccaletti, D. L. Valladares, J. Kurths, D. Maza, and H. Mancini, Phys. Rev. E **61**, 3712 (2000).
[30] J. D. Farmer, Phys. Rev. Lett. **47**, 179 (1981).
[31] A. S. Pikovsky, Sov. J. Commun. Technol. Electron. **30**, 85 (1985).
[32] H. Strogatz Steven, Nature (London) **410**, 268 (2001).
[33] S. Boccaletti and F. T. Arecchi, Europhys. Lett. **31**, 127 (1995).
[34] S. Boccaletti, C. Grebogi, Y. C. Lai, H. Mancini, and D. Maza, Phys. Rep. **329**, 103 (2000).
[35] P. Horowitz and W. Hill, *The Art of Electronics* (Cambridge University Press, Cambridge, England, 1989).
[36] S. Hayes, C. Grebogi, E. Ott, and A. Mark, Phys. Rev. Lett. **73**, 1781 (1994).
[37] E. Rosa, Jr., S. Hayes, and C. Grebogi, Phys. Rev. Lett. **78**, 1247 (1997).
[38] L. Glass, Nature (London) **410**, 277 (2001).
[39] D. Hoyer, O. Hoyer, and U. Zwiener, IEEE Trans. Biomed. Eng. **47**, 68 (2000).
[40] N. F. Rulkov, Phys. Rev. Lett. **86**, 183 (2001).